High-pressure batch reverse osmosis (RO) for zero liquid discharge (ZLD) in a Cr(III) electroplating process

Karimi, S.; Engstler, R.; Hosseinipour, E.; Wagner, M.; Heinzler, F.; Piepenbrink, M.; Barbe, S.; Davies, P.A.

DOI:
10.1016/j.desal.2024.117479

Desalination 580 (2024) 117479

Contents lists available at ScienceDirect

Desalination

journal homepage: www.elsevier.com/locate/desal

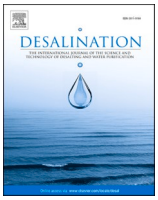

High-pressure batch reverse osmosis (RO) for zero liquid discharge (ZLD) in a Cr(III) electroplating process

S. Karimi [a], R. Engstler [b], E. Hosseinipour [a], M. Wagner [c], F. Heinzler [c], M. Piepenbrink [c], S. Barbe [b], P.A. Davies [a,*]

[a] School of Engineering, University of Birmingham, Edgbaston, Birmingham, UK
[b] Faculty of Applied Natural Sciences, Technische Hochschule Köln, Campus Leverkusen, Campusplatz 1, 51379 Leverkusen, Germany
[c] BIA Kunststoff- und Galvanotechnik GmbH & Co. KG, Solingen, Germany

HIGHLIGHTS

- First implementation of batch RO technology at high pressure of 120 bar
- Method for setting switch pressure in hybrid semi-batch/batch RO operation
- Cr(III) recovered from metal plating rinse water at industrial scale
- Concentration factor of 10–23 for Cr(III) achieved in a single process step
- Specific energy consumption of <2.25 kWh/m^3 and water recovery of 95 %

GRAPHICAL ABSTRACT

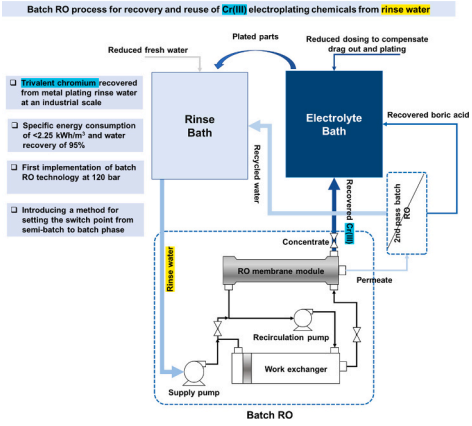

ARTICLE INFO

Keywords:
Batch RO
High-pressure RO
Energy saving
Metal plating wastewater
Trivalent chromium
Zero liquid discharge

ABSTRACT

A batch RO system was designed and built for high-pressure (120 bar) operation. The system was developed for a ZLD application involving treatment of metal plating wastewater from a Cr(III) electroplating process at a major industrial plant. Hybrid semi-batch/batch operation enabled a compact design to be achieved. To maximize water recovery without exceeding a set peak pressure, a method for controlling the switch point between semi-batch and batch phases was developed. The system was tested with feed representative of rinse water from the electroplating process. A range of feed concentrations (at 10–20× dilution of the plating bath), feed flows (0.21–0.46 m^3/h), water fluxes (6–14 LMH) and water recoveries (87–95.7 %) were investigated. The system successfully recovered Cr(III) and restored its concentration to that of the electrolyte bath, thus meeting the requirements for reuse in the electroplating process. Rejection of most species was >99.8 %, sufficient for reuse of the permeate as rinse. However, rejection of boric acid was only 69–80 % such that a second RO pass may be needed to remove boric acid. Specific Energy Consumption was <2.25 kWh per m^3 of treated rinse water, representing a 50-fold saving compared to the current method of treatment and disposal at the industrial plant.

* Corresponding author.
E-mail address: p.a.davies@bham.ac.uk (P.A. Davies).

https://doi.org/10.1016/j.desal.2024.117479
Received 20 December 2023; Received in revised form 14 February 2024; Accepted 24 February 2024
Available online 28 February 2024

Nomenclature

Symbols

A	m^2, Membrane area
A_m	LMH/bar, Membrane permeability
a_w	-, Water activity
c	mg/L, Concentration
c_f	mg/L, Feed concentration
c_p	mg/L, Permeate concentration
c_c	mg/L, Concentrate concentration
E_{rp}	kWh, Energy consumption of recirculation pump
E_{sp}	kWh, Energy consumption of supply pump
J	LMH (L/m^2/h), Water flux
k	bar.L/mg, Constant
n	osmol/kg, Osmolality
P	bar, Pressure
$P_{0,I}$	bar, Initial pressure for the first cycle
P_m	bar, Hydrodynamic friction of the membrane pores
P_{max}	bar, Maximum pressure
P_{switch}	bar, Switch pressure
pK_a	-, Acid dissociation constant
Q_p	L/min, Permeate flowrate
r	%, Water recovery
R_s	%, Rejection
R	J/(gmol.K), Universal gas constant
T	K, Temperature
V_0	L, Internal volume
V_{b0}	L, Feed volume during the batch phase
V_{back}	L, Osmotic backflow
V_{conc}	L, Purge volume
V_f	L, Feed volume
V_p	L, Permeate volume
V_s	m^3/gmol, Partial molar volume of water
V_{sb}	L, Feed volume during the semi-batch phase
η	-, Empirical pressure correction factor
π	bar, Osmotic pressure
ρ_w	kg/L, Water density

Abbreviations

CF	Concentration Factor
LMH	Litre per square Meter per Hour
MVC	Mechanical Vapor Compression
NF	Nanofiltration
PLC	Programmable Logic Controller
REACH	Registration, Evaluation, Authorisation and Restriction of Chemicals
RO	Reverse Osmosis
SEC	Specific Energy Consumption, electrical kWh per m^3 of treated wastewater
SI	Supporting Information
TOC	Total Organic Carbon
UF	Ultrafiltration
UV	Ultraviolet
ZLD	Zero Liquid Discharge

1. Introduction

Batch RO is an innovative approach to desalination that enables high recoveries to be achieved with modest energy consumption [1–5]. This makes it especially interesting for separation and recovery processes where zero or minimal liquid discharge is required. Several configurations of batch RO have been presented in the literature [6,7]. In principle, batch RO can achieve the theoretical ideal minimum specific energy consumption (SEC) of desalination [8]. In practice, however, there are several losses that affect its efficiency. Taking into account frictional losses and concentration polarization, Werber et al. [9] carried out a theoretical study to compare the performance of batch RO against several other RO configurations. These configurations included batch, semi-batch, and conventional staged RO processes. The study confirmed that, even considering losses, batch RO incurs the least SEC. However, true batch RO requires a large-pressurised vessel of variable volume, making it difficult to scale up. The size of this vessel increases with recovery ratio. Thus, while batch RO has been demonstrated at recovery of 80 % [2], at higher recovery practical implementation becomes difficult unless some modifications are introduced.

To overcome this difficulty, Park et al. [10] recently proposed a hybrid mode of operating batch RO that achieved similar SEC to true batch RO, while using a smaller pressurised vessel (i.e., work exchanger). Hybrid batch RO uses a preliminary semi-batch phase followed by a batch phase. The hybrid approach was later validated experimentally using brackish water feed, achieving in a single stage 95 % water recovery with SEC <0.6 kWh/m^3 [11]. Such high recovery has great potential for ZLD applications. Nonetheless, this experimental study [11] had some important limitations, namely: (1) because the batch RO system was rated at only 25 bar, it could not achieve high final concentrations, thus limiting its use in ZLD; and (2) no systematic method was presented for controlling the switch point between semi-batch and batch phases of operation, which (as this study will show) is an important consideration in high-pressure operation. In this study, we present a high-pressure (120 bar) batch RO system with water recoveries >95 % and we apply it to a challenging ZLD application in electroplating of chromium.

In general, electroplating processes tend to produce large amounts of environmentally-hazardous wastewater [12]. In the case of chromium, strict regulations limit concentrations in wastewater in most European countries. Limits range from 0.05 to 0.3 mg/L for hexavalent chromium, Cr(VI), and from 0.3 to 10 mg/L for total chromium content in effluents. Germany has especially strict regulations, limiting Cr(VI) to 0.1 mg/L and total chromium to 0.5 mg/L [13]. Electroplating also faces economic challenges [14]. According to the German Central Association for Surface Technology, the cost of chromium electroplating had increased by 52 % in 2021 compared to the mean over 2015–2017, reaching 11.98 €/m^2. This increase was driven by a 37 % increase in energy costs and a 63 % increase in metal costs [15]. The cost has recently increased further, reaching 17.17 €/m^2 [16]. Cr(VI) is carcinogenic and is being phased out in favour of trivalent chromium, Cr(III), as a less harmful alternative [17,18]. Nevertheless, Cr(III) still presents a significant environmental hazard. Moreover, it is more expensive than Cr(VI) in terms of the whole electrolyte composition and its maintenance, thus giving a strong incentive to recover and reuse Cr(III) waste.

In the Cr(III) plating process, parts are immersed in an electrolyte bath for the electrodeposition of chromium layers. The electrolyte contains a chromium source together with organic acids as complexing agents, boric acid as buffer, sulfates as conducting salts, plus other organic additives and surfactants to increase plating performance [19–21]. The parts are then rinsed of excess plating chemicals, generating a stream of wastewater.

Traditional thermal technologies consume substantial energy to treat such electroplating wastewater [22]. For example, Yang et al. [23] used mechanical vapor compression (MVC) and reported a SEC of 58 kWh/m^3. Common chemical treatment methods include hydroxylic precipitation which produces an insoluble metal sludge, which is separated by filtration [14]. Coagulation or flocculation agents are often used to improve the sedimentation or flotation of the sludge and reduce its settling time, which further increase the costs. Other treatments include

adsorption on powdered activated carbon or ion exchange resins. Electrochemical methods have also been investigated, including electrocoagulation, electrodeposition and electrodialysis; nonetheless, these may incur high capital and energy costs, and create new waste streams [24–26].

Membrane separation technologies have the potential to overcome such limitations. Their advantages include simplicity, cost-effectiveness, energy efficiency, and scalability. Membrane technologies – including ultrafiltration (UF), nanofiltration (NF) and reverse osmosis (RO) – have received increased attention for the removal of various metal ions [14,27]. Although RO has been used to remove Cr(VI) from wastewater [28–32], its use for Cr(III) rinse water treatment is quite new. To our knowledge, the only relevant study on Cr(III) is that of Engstler et al. [19] which used a conventional bench-top RO system in the laboratory. The study achieved the concentration factor needed for direct reuse of the electroplating chemicals. Nonetheless, the system was much too small for industrial implementation, comprising just 160 cm^2 of membrane and processing only a few litres of wastewater over several weeks. No measurements of SEC were taken or reported. Moreover, severe membrane fouling was observed which led to a halving of the membrane permeability, such that this system did not provide an industrial solution for Cr(III) wastewater treatment.

Because electroplating rinse water is very dilute, most of the water (~90–95 %) must be removed to restore the electrolyte concentration sufficiently for reuse. In the field of desalination, such a high percentage of water recovery is quite unusual and challenging. In seawater desalination by RO, for example, the water recovery is typically only about 45 % [33]. Increased recovery tends to increase the SEC of RO [34]. Meanwhile, energy saving is ever more important to the metal plating industry. This makes an energy-efficient approach, such as batch RO, attractive in this application.

Batch RO has been evaluated for seawater [35], brackish groundwater [2] and for agricultural runoff water [36]. But to our knowledge, it has not been studied for water reuse in the metal plating industry, nor has it been implemented at high pressure. Therefore, the goal here is to develop and test a full-scale batch RO system for Cr(III) recovery and water reuse. The specific objectives are:

(1) Develop an efficient, 120-bar batch RO system that can process industrial quantities of Cr(III) rinse water with SEC <2.5 kWh/m^3 and water recovery up to ~95 %.
(2) Present a method for setting the switch point from semi-batch to batch phase in hybrid operation, as needed for the automation of the process.
(3) Test the system with metal plating rinse water made up in the laboratory, and measure key performance parameters including concentration factor and rejection of the main electroplating chemicals, pressure, SEC, water recovery, permeate quality and flux.
(4) Assess fouling and durability of the RO membrane in this system.

These objectives are guided by an application that is representative of modern Cr(III) plating industry, as described in Section 2. Then, Section 3 explains the concept and development of the high-pressure batch RO technology. Section 4 presents the theory of the methods used to set the switch point. The experimental procedure, equipment and characterisation methods are given in Section 5 while Section 6 presents the results (including the assessment of fouling) and discusses how the findings compare with earlier works. Section 7 states the main conclusions of the study.

2. Industrial electroplating plant

The batch RO system has been designed to meet the requirements of the state-of-the-art Cr(III) plating process of BIA Kunststoff- und Galvanotechnik GmbH & Co. In the BIA plant, parts of ABS (acrylonitrile-butadiene-styrene) undergo several successive process steps separated by dedicated rinsing baths. Etching, activation, and acceleration steps first prepare the parts for metal electroplating by rendering the surface conductive. A thin 1–2 μm nickel layer is then applied to reinforce the surface, followed by a thick 20–30 μm copper layer to correct any unevenness and provide ductility. Next, another 7–10 μm of semi bright nickel is applied for corrosion resistance. Nickel is electroplated in two further steps to make the surface bright or satin and for more corrosion protection. To avoid cross contamination, thorough rinsing is applied to ensure that virtually all soluble nickel is removed from the parts. Finally, electroplating of a 0.3–0.8 μm layer of chromium generates a hard and chemically resistant surface. The finished parts are supplied mainly to the automotive industry.

The plant has three Cr(III) plating lines each including a 1.5-m^3 rinse bath (Fig. 1) which is emptied twice weekly, thus generating in total about 9 m^3 of chromium-contaminated rinse water per week. As the rinse water becomes contaminated by drag out from the electrolyte bath, it has similar composition to the electrolyte bath but diluted by a factor of 10–20 typically. As such, it contains 500–1000 mg/L of Cr(III) which greatly exceeds the allowed limit of 0.5 mg/L for wastewater discharge. Despite the high cost of the plating chemicals and their disposal, BIA (like other electroplating factories) has not yet been able to implement any effective recovery process. Currently, the rinse is disposed of by hydroxylic precipitation to form a $Cr(OH)_3$ sludge. However, an initial treatment by UV/H_2O_2 oxidation is needed to destroy the complexing agents. The UV lamps are energy intensive, and for this reason disposal currently incurs a SEC of 118 kWh of electricity per m^3 of wastewater. As shown in Fig. 1, it is now proposed to recycle both water and chemicals in this process, with the help of batch RO to achieve much lower SEC.

3. Batch RO system

The batch RO system was supplied by ETS Design Ltd., London (model number 477) and installed in the laboratory at the University of Birmingham (Fig. 2). The design was based on an earlier system also installed at the university [2] but with upgrades for the high-recovery and high-pressure operation needed for the metal plating wastewater treatment.

Unlike the earlier system, this system was designed from the outset to be operated in hybrid semi-batch/batch mode, thus avoiding the need for an excessively large work exchanger [10,11,37]. If non-hybrid batch

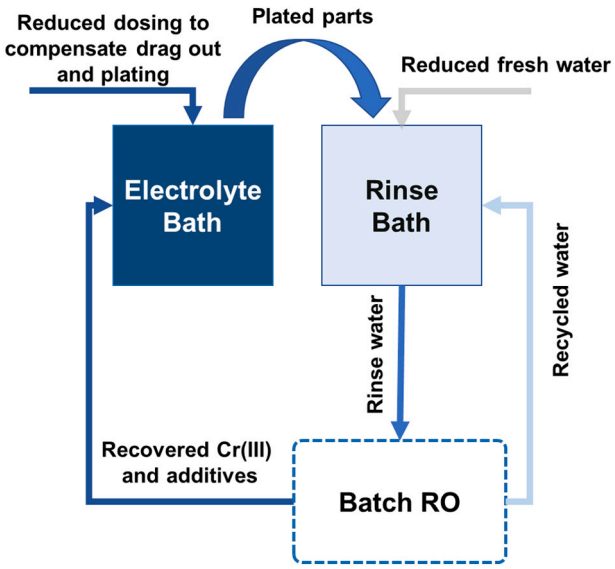

Fig. 1. Schematic of Cr(III) plating line at BIA, showing the electrolyte bath and rinse bath. The dashed box indicates the proposed recycling system using batch RO.

mode had been specified, a work exchanger volume of about 300 L would have been needed to achieve the required water recovery of 95 %. In hybrid operation, this volume is reduced to just 38.5 L without significant penalty in SEC [10]. This size reduction is especially important because of the space restrictions at the BIA factory where a similar system will later be installed. Moreover, though multi-stage conventional RO may be another option to achieve 95 % recovery, in practice this would likely require a 3-stage system with a large footprint and of capacity exceeding the requirements of this application. In contrast, the hybrid batch RO system provides a compact solution at the required scale.

Fig. 3 illustrates the concept of the system operating in hybrid mode. It includes two pumps: a supply pump, that provides a feed pressure of 120 bar, and a recirculation pump that operates under a high pressure but provides a low pressure rise to overcome internal pressure losses. It also includes three valves: the bypass, recirculation, and concentrate valve. Operation is cyclic involving three phases, i.e., semi-batch pressurization, batch pressurization, and purge-and-refill. The phase is determined by the state of the valves. In the semi-batch phase (Fig. 3a) the bypass and recirculation valves are open while the concentrate valve is closed. The piston is stationary at the left end of the work exchanger, resulting in a fixed internal volume. Wastewater is fed via the supply pump and mixed with concentrate returning from the RO membrane module, while the recirculation pump sends the mixed solution to the work exchanger. The solution then passes through the recirculation valve and the membrane module where permeate water exits such that the recirculating solution gradually becomes more concentrated.

At the end of the semi-batch phase, the system is switched to batch phase by closing the bypass valve while the other two valves remain in the same state (Fig. 3b). The switch causes the pressure to rise more sharply. In the absence of the bypass path, the high-pressure supply forces the piston to the right, thus decreasing the internal volume. This phase continues until the piston reaches the other end of the work exchanger. With the concentrate valve closed, the volume of permeate corresponds to that displaced by the piston. Finally, the purge-and-refill phase (Fig. 3c) is started by opening the concentrate and bypass valves and closing the recirculation valve. Now, the supply branches in two directions after the bypass valve. It displaces the concentrate from the RO module, which leaves the system via the concentrate valve. It also passes through the recirculation pump and refills the work exchanger. Pressure variations in semi-batch and batch phases of hybrid operation are shown in Fig. 4.

Preliminary measurements indicated that, depending on the type of electrolyte, the osmotic pressure of the electrolyte bath could reach 78 bar. To overcome this while providing sufficient net driving pressure, it was estimated that an applied pressure exceeding 100 bar may be required. In contrast, the earlier system was rated at only 25 bar because it was designed to treat only brackish water [11]. Even seawater RO systems and membranes are normally rated at only 80 bar. Nonetheless, some membrane manufacturers have recently introduced membranes rated at high pressures for ZLD applications. The membrane selected for this study is rated at 120 bar (a DuPont™ XUS180808, an 8-in. diameter, 1.016 m long spiral-wound polyamide thin-film composite membrane with active area of 30.6 m^2). This kind of high-pressure RO membrane and process is a recent innovation that introduces several challenges with respect to, for example, safety, sealing and membrane compaction [38].

To ensure operator safety and system integrity at such high pressure, the design includes several features. A pressure relief valve actuates at 120 bar, releasing pressure and tripping a safety relay. The relay then cuts off power to the supply pump and opens two pneumatic drain valves, thus releasing system pressure at three points. All pressurised components are housed in a transparent polycarbonate enclosure with doors interlocked to the safety relay (Fig. 2). The safety relay also responds to other fault conditions including manual intervention via the emergency stop buttons. All these features are designed to be failsafe, such that loss of electrical or pneumatic supply, or an open-circuit fault condition, will cause the equipment to default to its safe state in which the drain valves are open. The Supporting Information (SI) provides a detailed schematic of the batch RO system (Fig. S1) and lists its main components including the pumps, valves, sensors, and controls (Table S1). The system is controlled by a programmable logic controller (PLC).

4. Theory

An important consideration in the operation of the batch RO system is the criterion for switching from semi-batch to batch pressurization phase (see Fig. 3). If the switch is too early, insufficient concentration will occur for reuse of the electrolyte. If too late, the pressure will rise above the safe working pressure and the system will automatically shut down and require restarting. To avoid such difficulties, the following theory provides two methods for setting the switch point.

4.1. Concentration factor method

The first method sets the switch point according to a target concentration factor CF. This factor refers to the chromium concentration in the concentrate divided by that in the rinse water feed. Because the chromium is thoroughly rejected by the high-pressure RO membrane (as confirmed in Section 6.1) virtually all the chromium is collected in the concentrate. Thus, provided that the system is operating in a steady cyclic condition such that no chromium accumulates internally, *CF* is

Fig. 2. The installed pilot scale 120-bar batch RO system at the University of Birmingham, UK, showing 8-in. RO module (top) and work exchanger (bottom) inside safety enclosure.

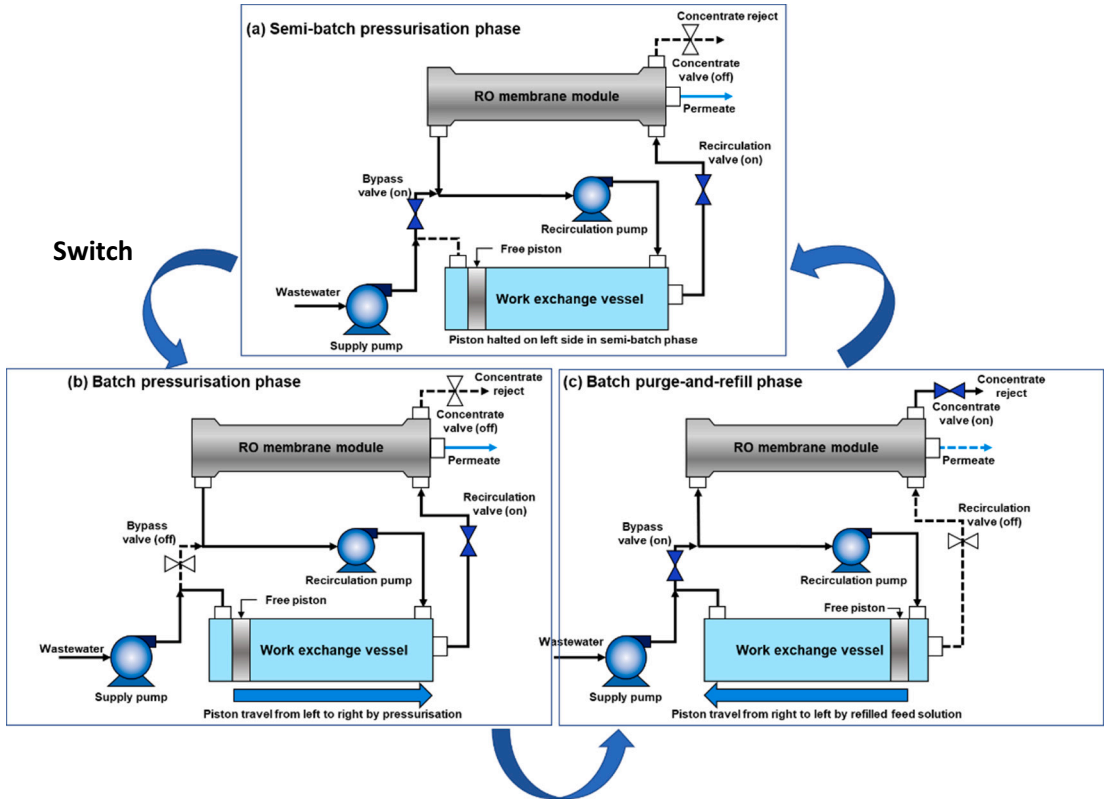

Fig. 3. Flow diagram and the working principle of the hybrid semi-batch/batch RO, showing the three phases of cyclic operation. The solid and dashed lines show flow and no flow, respectively.

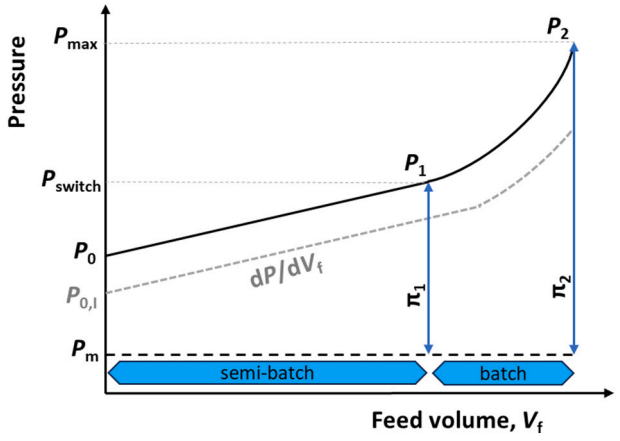

Fig. 4. Principle of determination of switch pressure based on pressure vs. feed volume. The dashed grey curve indicates the first cycle. Also showing the semi-batch and batch phases of hybrid operation, with the switch occurring at the end of the semi-batch phase.

calculated by dividing the volume V_f of rinse water fed to the system by the volume of concentrate, V_{conc}, collected from the system, i.e.

$$CF = \frac{V_f}{V_{conc}} = \frac{V_{sb} + V_{b0} + (V_{conc} - V_{back})}{V_{conc}} \quad (1)$$

where V_{sb}, V_{b0} , and $(V_{conc} - V_{back})$ are the feed volumes during the semi-batch, batch, and purge-and-refill phases respectively. V_{back} is the osmotic backflow [11]. Table 1 shows the volumes used in this study as determined by the design of the system.

Based on these volumes, eq. (1) becomes

$$CF = 3.1 + \frac{V_{sb}}{16} \quad (2)$$

Eq. (2) provides a criterion for the switch point based on setting V_{sb}, which is known from the change in mass (or level) of the feed tank. In other words, to achieve a target *CF* we need to supply:

$$V_{sb} = 16\,(CF - 3.1) \quad (3)$$

Eq. (2) shows that CF increases with V_{sb} from the minimum value of 3.1 at V_{sb}=0.

4.2. Peak pressure method

The second method addresses the risk of excessive pressure. The method relies on a minimum number of input parameters, making it simple to implement. It avoids the need for accurate characterisation of the rinse water feed.

According to the solution-diffusion theory, the applied pressure (P) in RO has two components, one corresponding to the hydrodynamic friction of the membrane pores (P_m) and the second corresponding to osmotic pressure (π). Thus:

$$P = P_m + \pi \quad (4)$$

The first component (P_m) is equivalent to the permeate flux (J) divided by the membrane permeability (A_m), i.e.

Table 1
Volumes of the high-pressure batch RO rig used in this study [L]. The osmotic backflow was based on the maximum value observed in an earlier study [2].

Feed volume batch phase (work exchanger swept volume)	V_{b0}	38.5
Concentrate volume	V_{conc}	16.0
Osmotic backflow	V_{back}	5.0
Internal volume	V_0	54.9

$$P_m = J/A_m \tag{5}$$

J is the permeate flowrate (Q_p) divided by the membrane area (A).

$$J = \frac{Q_p}{A} \tag{6}$$

where the permeate flowrate (Q_p) is the permeate volume (V_p) divided by the total duration of the semi-batch and batch pressurization phases. Therefore, P_m is proportional to the feed flow and is considered a constant for a series of cycles of the batch RO system (normally lasting less than one day) during which the feed flow and flux remain constant.

The osmotic pressure component in eq. (4) is related to the concentration, c, of the solute inside the batch RO system. Osmotic pressure increases with concentration and, at low concentrations such as those occurring during the semi-batch phase, the relation is expected to be linear according to a constant k. This constant lumps together factors such as the osmotic coefficient of the solute, temperature, rejection, and concentration polarization effects which are assumed approximately constant for a given series of cycles. Thus eq. (4) becomes:

$$P = P_m + kc \tag{7}$$

During the semi-batch phase, the internal volume of the system remains fixed at V_0 and solute is gradually added at concentration c_f via the feed stream which arrives at a flow rate of dV_f/dt where V_f is the volume of feed that has been added since the beginning of the phase. This accumulation of mass causes the concentration to rise with time, i.e.

$$V_0\frac{dc}{dt} = \frac{dV_f}{dt}c_f \tag{8}$$

This may be written as:

$$\frac{dc}{dV_f} = \frac{c_f}{V_0} \tag{9}$$

Because P_m is constant, eq. (7) can be differentiated with respect to V_f to give:

$$\frac{dP}{dV_f} = k\frac{dc}{dV_f} \tag{10}$$

Substituting from eq. (9) gives:

$$\frac{dP}{dV_f} = k\frac{c_f}{V_0} \tag{11}$$

Eq. (11) shows that the pressure is expected to rise linearly with feed volume at a rate proportional to the feed concentration (c_f). At the beginning of the first cycle of the batch RO operation, the system is initially filled with solution at the feed concentration. Therefore, the initial pressure ($P_{0,I}$) according to eq. (7) will be:

$$P_{0,I} = P_m + kc_f \tag{12}$$

where the second subscript 'I' indicates 'the first cycle'. Substituting from eq. (11) and rearranging for P_m provides:

$$P_m = P_{0,I} - V_0\frac{dP}{dV_f} \tag{13}$$

Eq. (13) allows the value of P_m to be determined from the slope and intercept of the pressure vs volume curve during the first cycle (see Fig. 4).

Next the batch phase is considered. During this phase, the volume of the system is decreased from V_0 by the swept volume V_{b0} of the work exchanger to give a final volume of $V_0 - V_{b0}$. Applied pressure increases from P_1 to P_2. This phase is approximately a constant mass phase, whereby the same amount of solute is compressed into a smaller volume, and osmotic pressure is expected to rise in inverse proportion to the volumetric ratio $(V_0 - V_{b0})/V_0$. Nonetheless, experiments have shown that the observed rise in pressure is slightly less than expected [11]. Reasons for this may include: (1) <100 % rejection such that the mass of solute decreases; (2) deflection of the membrane and dilation of the pressurised system; (3) sub-linear increase of osmotic pressure with concentration. Therefore, an empirical correction η (slightly less than one) is applied to account for these factors, as follows:

$$\frac{\pi_2}{\pi_1} = \eta\frac{V_0}{(V_0 - V_{b0})} \tag{14}$$

where π_1 and π_2 are the osmotic pressures at the beginning and end of the batch phase, respectively. Like P_m, η is initially unknown, but it can be found after each cycle based on measured pressures as follows:

$$\eta = \frac{(P_2 - P_m)}{(P_1 - P_m)}\frac{(V_0 - V_{b0})}{V_0} \tag{15}$$

η is assumed to remain approximately constant from one cycle to the next. The maximum osmotic pressure that can be utilised is the difference between the maximum allowable pressure and the hydrodynamic friction pressure, i.e.

$$\pi_2 = P_{max} - P_m \tag{16}$$

The corresponding switch pressure is given by:

$$P_{switch} = P_m + \pi_1 \tag{17}$$

Combining eqs. (14), (16), and (17) gives the following equation for the switch pressure according to the maximum pressure P_{max}:

$$P_{switch} = P_m + \frac{(P_{max} - P_m)}{\eta}\frac{(V_0 - V_{b0})}{V_0} \tag{18}$$

Alternatively, this can be rearranged to calculate P_{max} resulting from a given switch pressure:

$$P_{max} = \frac{\eta V_0(P_{switch} - P_m)}{(V_0 - V_{b0})} + P_m \tag{19}$$

Eq. (19) confirms the importance of precise adjustment of P_{switch}. This is because of the sensitive dependence of P_{max} on P_{switch} due to the multiplying factor of $V_0/(V_0 - V_{b0})$ which equals 3.35 in this study. For example, using typical values of $\eta = 0.8$, P_m=12 bar and the volumes in Table 1, a modest increase in P_{switch} from 35 to 55 bar increases P_{max} greatly from 70 to 120 bar.

To summarize, the peak pressure method is implemented as follows:

1. For the first cycle, a conservatively low value of P_{switch} is chosen to ensure that P_{max} is not exceeded. P_{switch} is calculated by eq. (18) with η=1 and P_m based on previous tests carried out at similar feed flow. If no such test result is available, eq. (5) may be used to estimate P_m using permeability based on data from the membrane manufacturer. The PLC program controls the system to switch phase when the applied pressure reaches P_{switch}.
2. At the end of the first cycle, eqs. (13) and (15) are used to find more precise values of P_m and η respectively (for example, η=0.8) based on the measured data of pressure vs. feed volume. Eq. (18) is then used to determine P_{switch} for the second cycle.
3. Following each subsequent cycle, an updated value of η is found using eq. (15) while P_m remains constant. Eq. (18) is again used to determine P_{switch} for the next cycle.

The two approaches to determining switch point (i.e., based on concentration factor or based on peak pressure) will be evaluated and compared in the experimental part of this study.

5. Materials and methods

5.1. Experimental setup

Fig. 5 shows the experimental set up including the batch RO rig, supply pump (CAT pumps, model 3CP1241G), plastic tanks (1500 L for

feed and permeate and 425 L for the concentrate tank), cartridge filter (Amazon Filters Ltd., Superpleat II 20 × 4.5-in. filter, 1 um) and sensors (see SI). The feed, permeate and concentrate tanks had scales (Mettler Toledo) to record the weight changes. Temperature of the feed tank was kept constant at 25 ± 0.5 °C using a thermostat and four immersed 650 W titanium heaters. The energy consumption of the supply pump was monitored using a power sensor (Multitek M100-WA4). Pressure was measured using a sensor on the feed line (Applied Measurements LTD, P600). The peak pressure of each cycle was recorded at the end of the batch pressurization phase, when the highest concentration of concentrate leaves the membrane module. A data logger recorded measurements from the sensors and scales at intervals of approximately one second. Raw experimental data are included as supplementary files (see SI Section 4).

5.2. Rinse water preparation

The rinse wastewater was prepared by dilution of the electrolyte bath solution to replicate the composition at the BIA plant. The electrolyte bath solution was synthesized using the TRILYTE® FLASH SF-POP products and procedure supplied by MacDermid Enthone (Birmingham, UK) [39]. TRILYTE® FLASH SF-POP is a REACH compliant, corrosion resistant Cr(III) plating process providing a direct substitute for Cr(VI)-based solutions. It is used for the deposition of a bright decorative chromium layer over bright or satin nickel layers [40]. The products are listed in Table 2 together with their functions and the quantities used.

The electrolyte bath solution was synthesized first by adding 65 L of tap water to the feed tank. Then, the TRILYTE FLASH SF Makeup was added followed by heating the solution using the immersion heaters to 65–70 °C. Next, 23 Kg of TRILYTE FLASH SF Buffer was added in portions while vigorously stirring using a recirculation pump. This step was done very carefully to ensure that all the salts are dissolved. 2 kg of potassium hydroxide 50 % wt. (Fisher Scientific) was then added to the solution to adjust the pH to 3.5–3.9. Thereafter TRILYTE FLASH SF, Replenisher and TRILYTE WETTING AGENT were added and the water level topped up to 120 L. The measuring was done using the weighing platform beneath the tank (component density values were used to convert volumes to mass). Finally, a series of representative electroplating rinse water bath compositions were prepared by dilution with tap water by a factor of 10, 15, and 20× respectively. These compositions were used as the feed to the batch RO in the experiments described next.

5.3. Experimental procedure

To investigate performance over a range of feed concentrations, fluxes, and recoveries, two series of experiments were carried out: the first at set concentration factor and the second at set peak pressure

Table 2
Commercial products used to make up 120 L of the TRILYTE® FLASH SF-POP electroplating bath solution, based on [39].

Commercial product	Quantity	Main function
TRILYTE FLASH SF Makeup	36 L	Source of chromium (III) and complexing agent [41]
TRILYTE FLASH SF Buffer	23 kg	Source of conductive salts and pH stabiliser (boric acid) [19–21,42,43]
TRILYTE FLASH SF Replenisher	2.4 L	Provides bright deposits [42,44]
TRILYTE WETTING AGENT	0.12 L	Reduces surface tension [42,45]

(following Sections 4.1 and 4.2 respectively). Experiments were conducted for at least three cycles and the measurement were done on the third cycle, as three cycles were enough to approximate steady state (see Fig. S2). Fluxes were adjusted over a range of 6–16 LMH by varying the speed of the supply pump. The recirculation flow, as measured by the flow sensor at the inlet to the recirculation pump, was adjusted to 6 times the supply flow. For further details of the experimental procedure the reader is referred to previous work [2].

The results from the experiments were obtained as follows. The permeate volume (V_p) and feed volume (V_f) were measured according to weight changes of the tanks, dividing by the solution density. The density of 1 kg/L was used throughout because the dilute nature of the feed and permeate caused their densities to be within 2 % that of pure water. Water recovery r was calculated as the ratio:

$$r = \frac{V_p}{V_f} \tag{20}$$

For components where rejection is nearly 100 %, the mass balance gives the concentration factor CF as the ratio of the volume of concentrate ($V_f - V_p$) to the volume of feed (V_f). Therefore, CF was calculated by:

$$CF = \frac{1}{1-r} \tag{21}$$

The electrical SEC was calculated as the sum of the energy consumption of the supply pump (E_{sp}) and recirculation pump (E_{rp}), divided by the feed volume over a whole cycle:

$$SEC = \frac{E_{sp} + E_{rp}}{V_f} \tag{22}$$

Rejection (R_s) was calculated by:

$$R_s = \frac{c_f - c_p}{c_f} \tag{23}$$

where c_f and c_p are the concentrations of a given ion in the feed and permeate respectively.

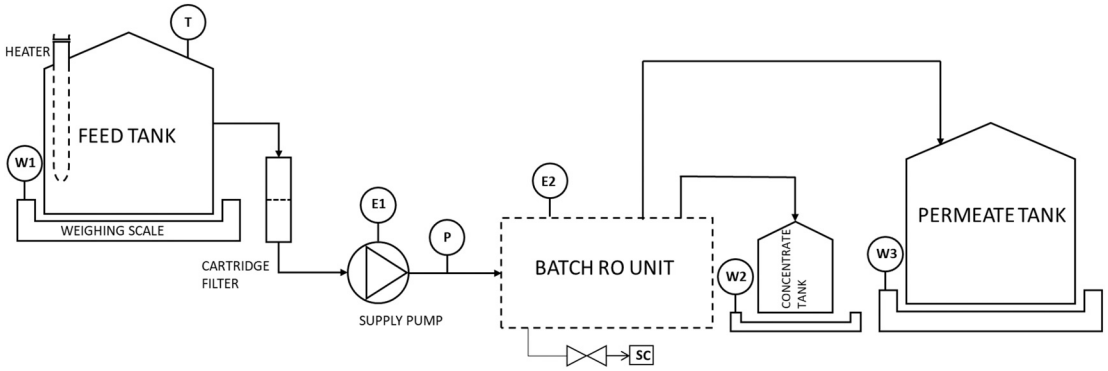

Fig. 5. Experimental set up. Symbols T, W, E and P indicate respectively temperature, weight, power, and pressure sensors.

5.4. Analytical methods

Inductively coupled plasma optical emission spectroscopy (ICP-OES) was used to determine concentrations of chromium, sulfate, boric acid in the feed and permeate. Further details are given in SI section 2, which also describes the determination of Total Organic Carbon (TOC) and measurement of osmotic pressure.

6. Results and discussion

6.1. Permeate concentrations and rejection

Chromium, sulfate, and TOC were detected in only small amounts in the permeate with maximum concentrations of 1.13, 13.28, and 0.053 mg/L respectively, as such well within the recycling limits for the rinsing bath of 10, 150, 100 mg/L respectively (see Table 3). In contrast, the concentration of boric acid in the permeate was ca. 1000–2000 mg/L, which was above the estimated allowed limit of 1000 mg/L.

Corresponding to these concentrations, the average rejections of chromium, sulfate, boric acid and TOC were 99.88, 99.85, 74.97, and 100 % respectively (see Table 3). Except for boric acid, all these rejections were therefore >99.8 %, as expected in RO for such multivalent ions and large organic molecules. Due to the high rejection of chromium, the permeate appeared very clear, whereas the concentrate was dark blue, compared to the light blue colour of the rinse water feed (see Fig. 6).

Rejection of boric acid was, however, only 69–80 %. This can be explained by the neutral character of the boric acid molecules at the working pH of 3.0–3.9 which is well below the pKa of 9.22. Therefore, the small uncharged and non-hydrated boric acid molecules can pass through the membrane to some extent [46]. Additionally, boric acid forms hydrogen bridges with the active groups of membranes and diffuses like water [47]. To ensure the required purity of the rinse water for reuse, the rejection needs to be improved to about 85 %. This could be achieved by adding a second RO pass (as indicated in the Graphical Abstract).

6.2. Performance at set concentration factor

The results of this section were obtained using the switch point method based on target concentration factor, as described in Section 4.1. Because of the high rejection (except for boric acid) concentration factor is directly related to water recovery via eq. (21).

Feed pressures (peak and average) and concentration factor as a function of recoveries of 87–95 % and at fluxes of 6–12 LMH are illustrated in Fig. 7a, b and c for dilutions of 10×, 15× and 20× respectively. To meet the requirement for recycling as defined by the plating industry, the target is 80–120 % of the initial concentration of the electrolyte bath [39]. Therefore, concentration factors of 8–12, 12–18, and 16–24 are needed for dilutions of 10, 15, and 20× respectively. These limits are shown by dashed horizontal blue lines in Fig. 7. The concentration factors presented are for the fully rejected components i.e., all components except boric acid, where lower concentration was achieved due to only partial rejection being achieved. Based on mass balance, boric acid concentration reached only 30–78 g/L – below the 80–110 g/L required for the electrolyte bath [39]. Boric acid would therefore need to be replenished or recovered further in a second RO pass. For the other components, sufficient concentration factors were achieved by working at high recovery, at fluxes up to 12 LMH.

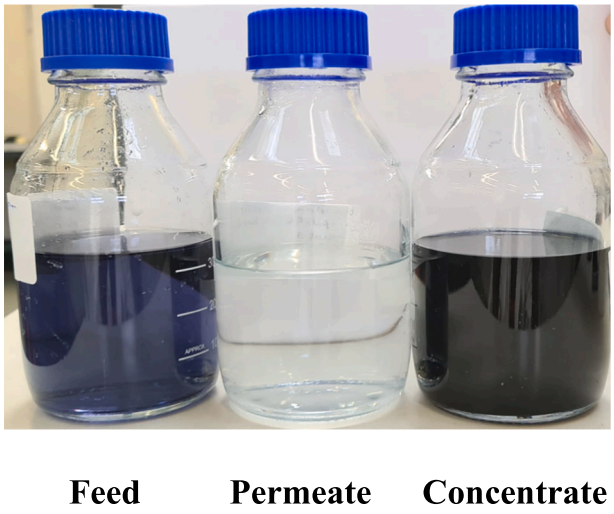

Fig. 6. Feed (dilution of 15×), permeate and concentrate samples (water recovery of 94.1 %, flux 6.6 LMH).

Note that, with this method of controlling switch point, there was no systematic way to ensure that the maximum system pressure of 120 bar was not exceeded. The maximum water recoveries and concentration factors had to be determined by trial and error.

As expected, peak and average pressure increased with water recovery and flux. At the highest recoveries and concentration factors, the average feed pressure was about half the peak pressure, and below the osmotic pressure of the concentrate. In contrast, a conventional single-stage RO system would require a constant feed pressure above the concentrate osmotic pressure to maintain a positive net driving pressure and transmembrane flux. These results suggest that the batch RO system has a significant energy advantage compared to conventional single-stage RO. Nonetheless, further experimental studies will be needed to make a complete and fair comparison, considering factors such as flux distribution, membrane friction, and salt retention in each system [48]. In addition, pump efficiency has an important effect on overall performance and may vary between batch and continuous systems.

The osmotic pressure of the final concentrate is an indication of the total concentration of final concentrate product, and it is higher than 47 bar for the samples that met the concentration requirement (Fig. 7). This osmotic pressure is at least 10 bar below that of the electrolyte bath (63 bar) mainly because of the loss of boric acid to the permeate.

Fig. 8 shows SEC < 2.15 kWh/m^3 when treating rinse water at a rate

Table 3
Rejections of chromium (III), sulfate, TOC and boric acid as a function of water recovery and flux, for dilution of 15×. Feed concentrations of chromium (III), sulfate, TOC and boric acid were 672.5, 6133, 575.1, and 6495 mg/L respectively.

Water recovery (%)	Flux (LMH)	Permeate concentration (mg/L)				Rejection (%)			
		Cr(III)	Sulfate	TOC	Boric acid	Cr(III)	Sulfate	TOC	Boric acid
88.4	6.5	0.68	7.12	0.053	1708.7	99.90	99.88	99.98	73.69
90.4	6.6	0.96	11.63	0.002	1805.2	99.86	99.81	100.00	72.20
94.1	6.6	1.13	13.28	0.000	2008.2	99.83	99.78	100.00	69.08
87.9	8.3	0.61	5.88	0.000	1480.9	99.91	99.90	100.00	77.20
90.3	8.3	0.82	8.82	0.000	1609.0	99.88	99.86	100.00	75.23
87.6	10	0.75	8.74	0.000	1285.4	99.89	99.86	100.00	80.21
90	10	0.69	6.98	0.000	1482.7	99.90	99.89	100.00	77.17

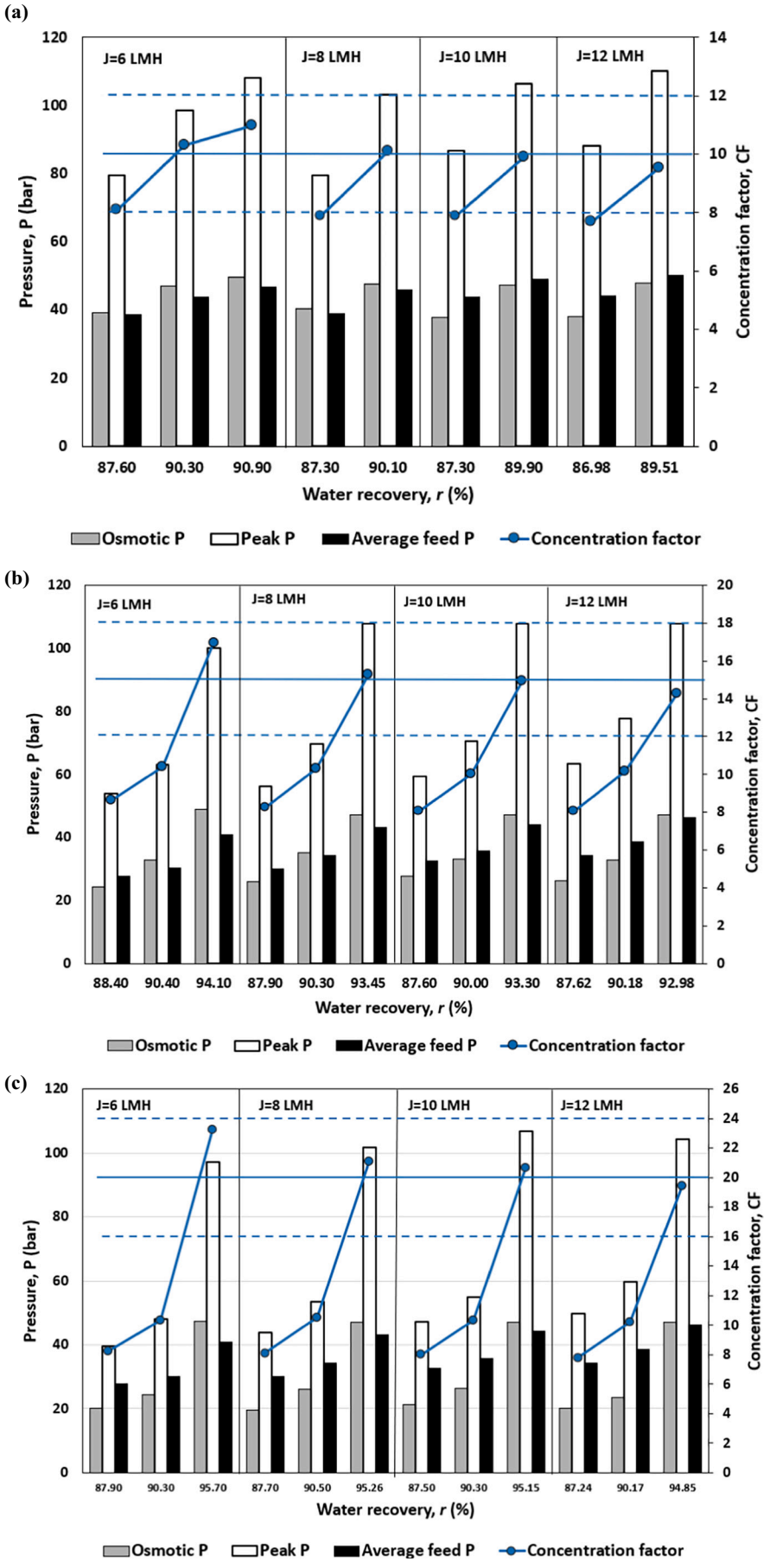

(caption on next page)

Fig. 7. Osmotic pressure of concentrate, peak feed pressure (P_{max}), and average feed pressure, at different water recoveries from 87 to 95 % and fluxes from 6 to 12 LMH for dilution of (a) 10×, (b) 15×, and (c) 20×. Osmotic pressure of feed was measured to be 7.55, 5.23 and 4.13 bar for dilutions of 10×, 15×, and 20× respectively. Also shows concentration factor, with dashed horizontal blue lines showing the lower and upper limits for recycling to the electrolyte bath, and the solid blue line showing the optimum value for recycling to the electrolyte bath.

of 0.21–0.42 m^3/h. Thus, it will be possible to treat 1.7–3.4 m^3 of rinse water in an 8-h working shift, meeting the requirement of the industrial process at BIA. SEC increased with water recovery and flux.

6.3. Analysis of results against the switch pressure theory

To assess the accuracy of the theory described in Section 4, the theory was used to analyse the above data. In total, 24 experiments were analysed covering fluxes of 6–12 LMH, water recoveries of 87–95 % and dilutions of 10, 15 and 20×.

The P_m value was calculated using eq. (13) (based on the recorded pressures in cycle 1) and is shown as a function of flux in Fig. 9a. In the semi-batch phase, dP/dV_f values were calculated for all three cycles. There was <10 % deviation in dP/dV_f at cycle 3 compared to cycles 1 and 2. The value at cycle 3 was plotted as a function of feed concentration as presented in Fig. 9b which shows the linear dependency of the dP/dV_f value to the feed concentration as predicted by eq. (11).

The peak pressure of the third cycle is predicted using eq. (19), based on the measured switch pressure and the value of η calculated from the previous cycle using eq. (15). This predicted peak pressure is compared against the measured value at cycle 3 to give a model error of <3 % (see Fig. 10). Fig. 10 also confirms that η has values consistently just below one (from 0.75 to 0.82) as assumed in the theory of Section 4.

6.4. Performance at set peak pressure

This section evaluates the method of setting switch pressure for a target peak pressure, as described in Section 4.2. In addition, the method is used to compare batch RO performance at 80 bar vs. 120 bar.

Experiments were carried out at dilutions of 15 and 20×, fluxes of 8–16 LMH, and two target peak pressures: (1) 108 bar to provide a 10 % safety margin below the maximum allowable pressure of 120 bar; (2) 72 bar to represent 80 bar maximum pressure as allowed by standard seawater RO membranes. Table 4 shows the results, including maximum obtained pressure at each cycle. In all cases, the peak pressure converged quickly from cycle 2 on, with ≤2.2 % deviation from the set peak pressure.

Fig. 11 presents three examples of pressure vs. feed volume, showing the value of η for each cycle. Cycle 1 had lower peak pressure due to the conservative setting of η_1=1 and the absence of salt retention, but the uniformity of η from cycle 2 onward means that switch pressure, water recovery, and concentration factor all converged rapidly. The linear increase of pressure in the semi-batch phase agrees with eq. (11).

The concentration factor at feed concentration of 15× is plotted versus flux, at both 80 and 120 bar maximum pressure, in Fig. 12. The optimum concentration factor of 15, needed to restore the electrolyte bath concentration, is shown by the solid blue line. The desired range of concentration factor of 12–18, corresponding to 80–120 % of the electrolyte bath concentration, is shown by dashed blue lines. The results show that batch RO was able to concentrate the Cr(III) rinse water sufficiently at fluxes up to 14 LMH at 120 bar operation, but unable to do so at 80 bar operation even at lower flux.

Compared to the method of 4.1, where switch point is set for a target concentration factor, this method automatically concentrates the wastewater to the maximum extent possible for a given flux and pressure limit, without the need for trial and error. It also avoids the need for accurate characterisation of the wastewater, as the concentration is effectively detected from the slope of pressure vs. feed volume during the semi-batch phase. This method is therefore recommended whenever

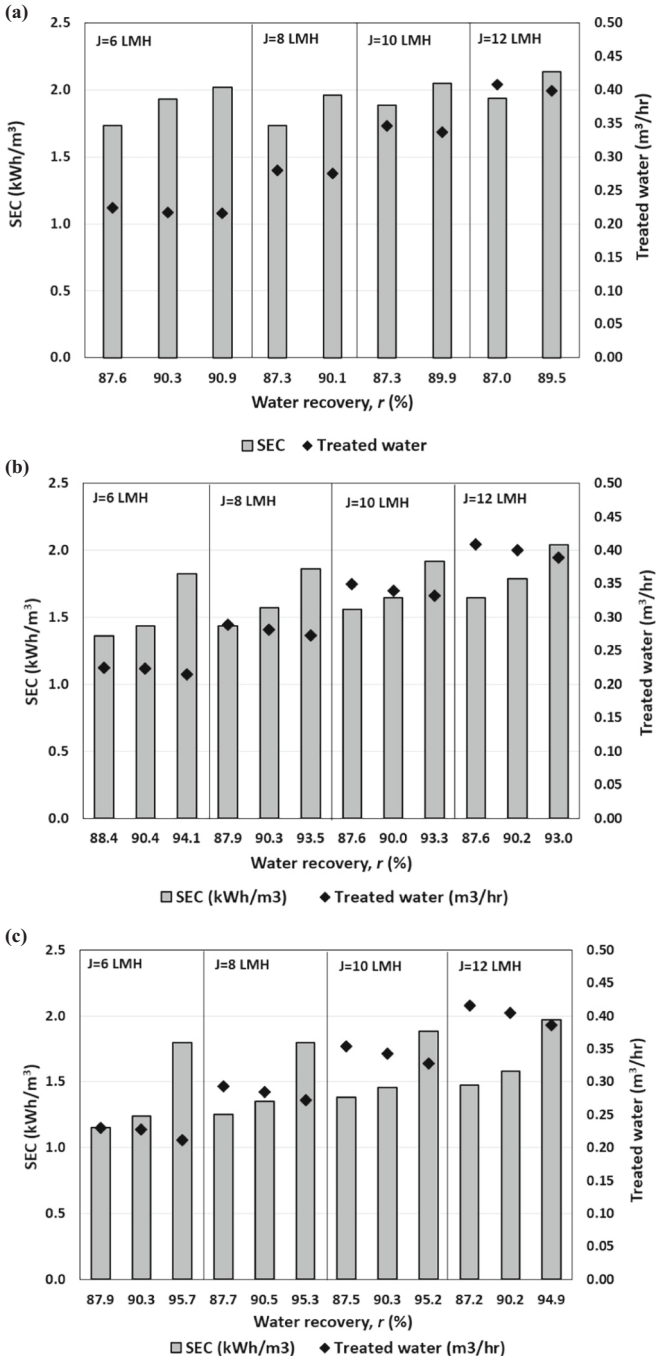

Fig. 8. Specific energy consumption (SEC) and flowrate of treated water at recoveries of 87–95 % and fluxes of 6–12 LMH for dilution of (a) 10×, (b) 15×, and (c) 20×.

there is a risk of approaching the maximum operating pressure of the system. In fact, the two methods of switch point control are complementary and can be used together. Thus, we recommend that the first method can be used to determine a supply volume in the semi-batch phase for a target concentration factor, while the second method is

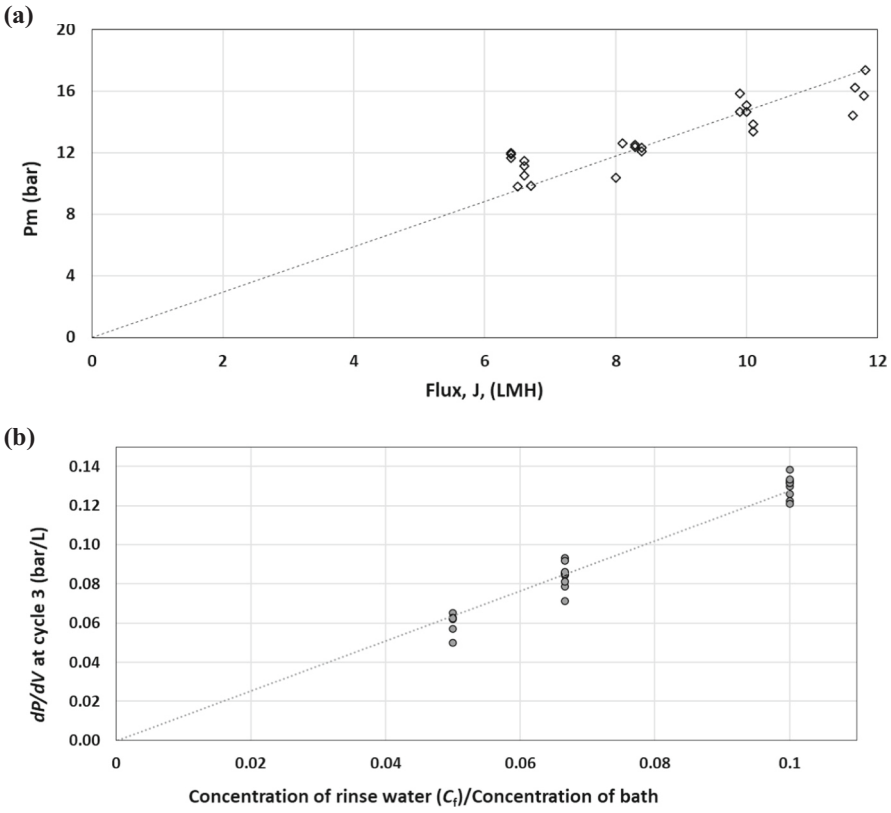

Fig. 9. Verification of theory of switch point determination, using results from Section 6.2: (a) Hydrodynamic pore friction pressure P_m as a function of flux J. (b) Slope dP/dV during cycle 3 of the semi-batch phase versus the relative feed concentration.

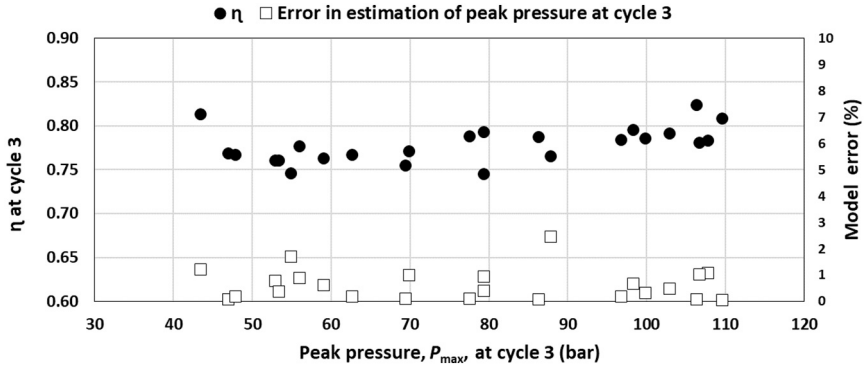

Fig. 10. Empirical pressure correction factor η and error of modelling peak pressure at cycle 3, at different peak pressures (cycle 3).

Table 4
The summary of the results obtained from the RO experiments operated using the methodology of switch pressure determination for a target peak pressure.

Dilution	Pressure limit (bar)	Target pressure (bar)	Flux (LMH)	Observed peak pressure (bar) at cycle:				Max deviation of peak pressure from target Cycles 2–4 (%)	Switch pressure Cycle 3 (bar)	SEC Cycle 3 (kWh/m^3)
				1	2	3	4			
15×	120	108	8	88.4	108.5	109.0	105.8	2.20	47.9	1.97
15×	120	108	10	90.0	107.7	107.2	107.5	0.50	48.8	2.00
15×	120	108	12	92.6	106.3	106.3	108.9	1.70	50.6	2.05
15×	120	108	14	89.5	108.9	107.7	107.6	0.87	51.0	2.22
15×	120	108	16	90.9	108.0	107.7	107.7	0.32	53.1	2.21
15×	80	72	8	58.3	72.0	71.5	71.7	0.50	34.6	1.54
15×	80	72	10	58.8	70.4	71.7	72.0	1.55	36.1	1.63
15×	80	72	12	63.1	71.3	71.6	71.7	0.65	36.8	1.71
15×	80	72	14	61.1	70.6	70.6	70.4	1.53	37.8	1.89
20×	120	108	12	88.6	109.2	107.7	–	1.24	49.9	2.04
20×	120	108	14	93.4	108.9	107.4	–	0.91	51.4	2.19

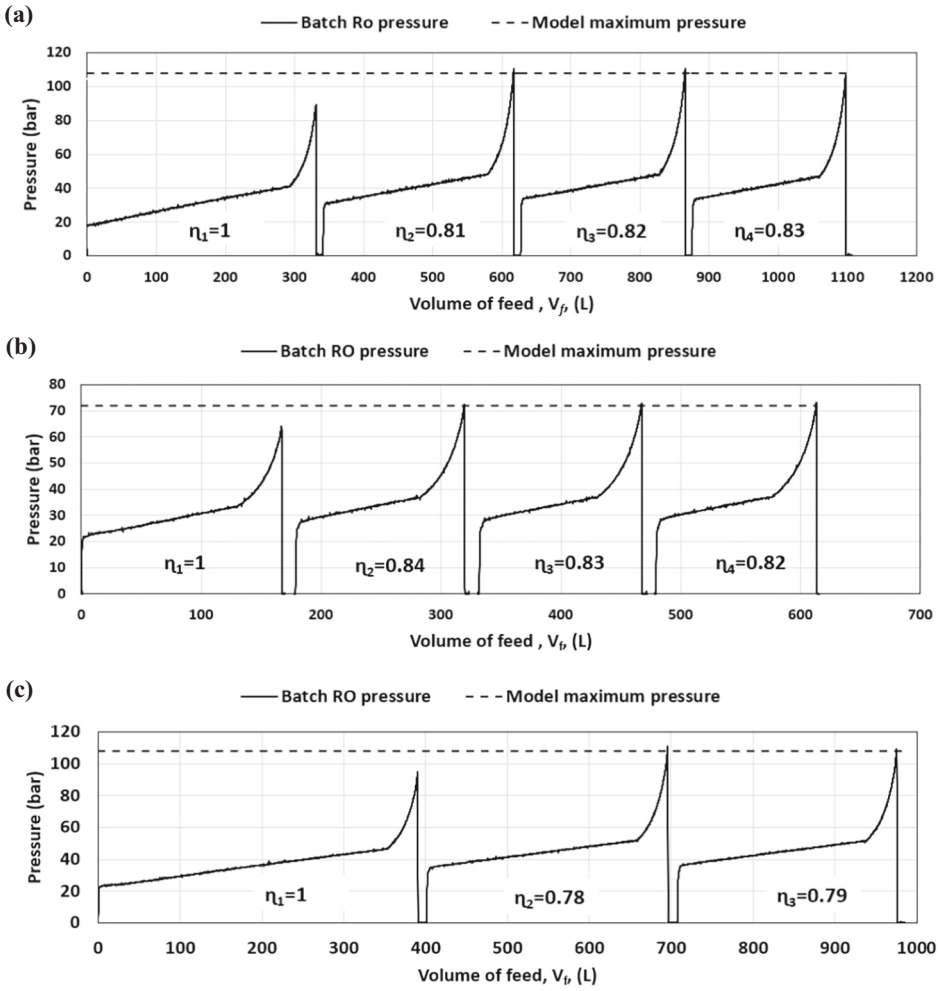

Fig. 11. Pressure variation vs. supplied feed volume for three experiments, using switch point setting based on peak pressure. (a) dilution of 15×, flux of 8 LMH, concentration factor of 15.48, set peak pressure of 108 bar (b) dilution 15×, flux 12 LMH, concentration factor 9.12, set peak pressure 72 bar, (c) dilution 20×, flux 12 LMH, concentration factor 18.34, set peak pressure 108 bar. Dashed horizontal lines show the set peak pressures.

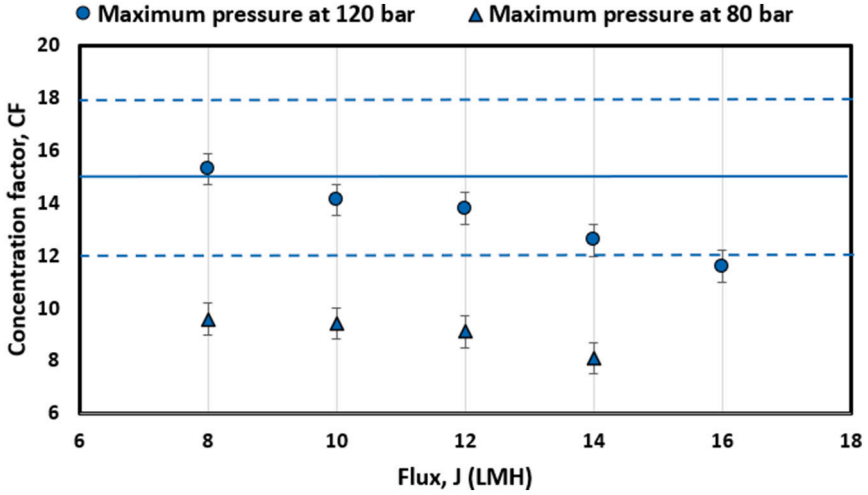

Fig. 12. Concentration factor vs. flux at 80 and 120 bar operation, for feed concentration of 15×. Dashed horizontal blue lines show the lower and upper limits for recycling to the electrolyte bath; the solid blue line shows the optimum for recycling to the electrolyte bath.

simultaneously used to set a safeguard on the switch pressure to ensure maximum system pressure is not exceeded. In this way, the switch will occur at whichever point is reached earlier (i.e., according to the target concentration factor or according to the pressure limit). If, however, the aim is simply to maximise concentration factor, then the first method is not needed.

6.5. Membrane fouling and durability

Total organic carbon (TOC) was present in significant quantities in the Cr(III) rinse water (at 926, 575, and 445 mg/L for feed dilution of 10,15, and 20× respectively) and could cause fouling of the RO membrane, as was previously observed in benchtop RO experiments with Cr (III) rinse water [19]. Membrane fouling can generally be detected by a decrease in flux, a decrease in permeability, and an increase in working pressure [49].

Membrane fouling and durability were investigated through two tests, each conducted before and after the entire series of Cr(III) experiments which lasted about 100 h in total. The first test was for permeability, using tap water in continuous flow mode at water flux of 17 LMH. The permeability tests showed negligible change in permeability and average pressure which were constant at 1.15 LMH/bar and 14.9 bar respectively. The second test was for salt rejection, using a feed solution of 4500 mg/L sodium chloride in hybrid semi-batch/batch mode, with water flux of 16.8 LMH and set water recovery of 0.94. The rejection showed a reduction of just 0.1 % from 96.7 % to 96.6 %. These results indicated negligible fouling and negligible deterioration in membrane performance. The absence of fouling tends to confirm previous work describing mechanisms of fouling avoidance in batch RO. These mechanisms may include periodic flushing, feed flow reversal, osmotic backflow, and salinity cycling [4,50].

6.6. Comparison against earlier studies

Table 5 compares the findings of this study against earlier studies on chromium plating rinse water treatment using RO technology. The comparison is limited to studies using the real composition of rinse water as occurring in modern metal plating plants, as opposed to simplified compositions that may omit important components.

Only this study used a RO membrane rated at 120 bar, whereas earlier studies used standard membranes limited to 80 bar or less. This higher working pressure enabled the process to achieve the required concentration for reuse while working at flux up to 14 LMH. The high water recovery of 87–95 % resulted in a chromium concentration factor of 8–23 thus going above the range of earlier studies. In addition, this study produced the highest output compared to other studies, making the system suitable for direct industrial application. Most earlier studies used Cr(VI), which is less challenging than the Cr(III) rinse water, because of the absence of other chemicals such as boric acid.

This study resulted in a SEC of 1.15–2.22 kWh per m^3 of treated wastewater corresponding to <2.42 kWh per m^3 of permeate water. None of the above studies reported SEC against which to compare. However, the SEC of traditional RO used in ZLD systems is reported to be 2–6 kWh/m^3. MVC, the most common thermal technique for ZLD, is highly energy intensive with SEC of 20–25 kWh/m^3 [51,52].

The flux in this study was higher than in the other Cr(III) study, but lower than in the Cr(VI) studies. This is because of the need to overcome higher osmotic pressures of the Cr(III) solution caused by the presence of additional components.

6.7. Future research

Longer term testing is needed to assess fouling and durability in the industrial application and to define clean-in-place procedures that may be required. Post treatment for improved boron rejection may be investigated using a second RO pass. Another important area of future study is modelling of the boron permeability in RO membranes in the batch RO process. Advances in membranes could be useful to improve to boron rejection. They could also be useful to reduce further the SEC of the batch RO process [53].

It will also be useful to update the previous mathematical model [2,11] of batch RO to predict behaviour and to design systems for a range of metal plating processes involving complex solutions. The simplified modelling presented here is only for the purpose of setting the switch point, and does not predict performance parameters such as SEC and rejection. Future research should also investigate the use of batch RO to treat rinse water containing other metals used in electroplating, such as copper and nickel. Moreover, future modelling and experimental studies may also address the issue of comparison between batch RO and multi-stage continuous RO systems that can also be used to achieve high recovery.

A further area of future research should be to explore the economic feasibility of batch RO in the metal plating wastewater application. In

Table 5
Performance comparison among relevant studies on chromium plating wastewater treatment using RO technology.

Main component and concentration in feed (mg/L)	Treatment method	Specific Energy Consumption (kWh/m^3)	Chromium concentration factor	Water output (m^3/h)	Flux (LMH)	Max Pressure (bar)	Reusability of concentrate	Reference	Comments
Cr(VI) 1800	UF/RO	Not reported	13.26	0.03	–	46	Yes	[31]	Rejection of 98.6 % for chromium. Flux not reported.
Cr(VI) 1.9	RO	Not reported	3.33	0.07	5–15	8	No	[30]	UF pretreatment. Metal, organic/inorganic compounds removed by RO with effectiveness 91.3–99.8 %. RO permeate reuse investigated.
Cr(VI) 100–1000	RO	Not reported	4.5	0.125	30–60	60	No	[29]	Rejection <98 % for concentration of 1000 mg/L. RO concentrate used to enable recovery of heavy metals through the ferrite process and ion exchange. Severe scaling observed.
Cr(VI) 84–228	NF/RO	Not reported	20	0.1	40–55	30	No	[28]	UF pretreatment. Permeate met requirements for reuse in rinsing bath.
Cr(III) 770	RO	Not reported	10.9	1.2×10^{-4}	3.75–7.5	80	Yes	[19]	Severe fouling observed.
Cr(III) 520–1080	Batch RO	<2.25	8–23	0.2–0.46	6–14	120	Yes	This study	Rejection >99.8 % for chromium. No fouling

addition, a life cycle assessment (LCA) should be carried out to assess fully the environmental impacts and benefits of this technology.

7. Conclusions

In this study, a high-pressure batch RO system has been developed for an industrial ZLD application involving the treatment of Cr(III) rinse water. The main conclusions are:

- The system was designed for safe and reliable operation at 120 bar. Hybrid semi-batch/batch operation avoided the need for an excessively large work exchanger, thus enabling a compact design.
- An approach to setting the switch point from semi-batch to batch phase was introduced and experimentally validated. This enabled the peak pressure to be controlled to within 2.2 % of a target value.
- The system provided >99.8 % rejection of Cr(III), sulfate, and organics, such that the permeate was sufficiently free of these species for reuse in the rinse bath.
- Nonetheless, rejection of boric acid was only about 75 %, such that a second RO pass may be needed to avoid boric acid contamination in the recycled rinse water.
- The batch RO system concentrated the rinse water sufficiently for reuse of Cr(III), sulfate, and organics in the electrolyte bath, providing 99.8 % rejection of these species. At 120 bar, a concentration factor up to 23 was achieved, thus meeting the target for reuse. In comparison, 80 bar operation did not reliably achieve a sufficient concentration factor.
- Working at fluxes of 6–14 LMH, the system treated 0.21–0.46 m^3/h of rinse water, meeting the requirements of the industrial electroplating process.
- SEC was 1.15–2.22 kWh per m^3 of treated wastewater, which is very competitive in the field of RO, and greatly superior to thermal methods, or to alkaline precipitation with UV pretreatment. In the industrial plant considered in this study, the new batch-RO process will reduce energy consumption by a factor of 50.
- No deterioration in membrane permeability or rejection occurred after 100 h of testing, indicating absence of fouling.

In summary, the high-pressure batch RO process provides an energy-efficient, compact and robust solution to the previously unsolved problem of treating and recycling Cr(III) waste at industrial scale.

CRediT authorship contribution statement

S. Karimi: Writing – original draft, Methodology, Investigation, Formal analysis, Conceptualization. **R. Engstler:** Writing – review & editing, Writing – original draft, Methodology, Investigation. **E. Hosseinipour:** Writing – review & editing, Writing – original draft, Methodology, Investigation. **M. Wagner:** Writing – review & editing, Investigation, Conceptualization. **F. Heinzler:** Writing – review & editing, Conceptualization. **M. Piepenbrink:** Writing – review & editing, Investigation. **S. Barbe:** Writing – review & editing, Funding acquisition, Conceptualization, Supervision. **P.A. Davies:** Writing – review & editing, Supervision, Methodology, Funding acquisition, Conceptualization.

Declaration of competing interest

The authors would like to declare that a spinout company (Salinity Solutions Ltd) was formed to exploit the batch RO technology, and that one of the authors (PAD) has an equity stake in this company.

Data availability

Raw data are included as supplementary files

Acknowledgement

This project has received funding from the European Union Horizon 2020 research and innovation programme under grant agreement No 958454. We also acknowledge the assistance of Marcus Allard of ETS Design Ltd.

Appendix A. Supplementary data

Supplementary data to this article can be found online at https://doi.org/10.1016/j.desal.2024.117479.

References

[1] D.M. Warsinger, E.W. Tow, K.G. Nayar, L.A. Maswadeh, Energy efficiency of batch and semi-batch (CCRO) reverse osmosis desalination, Water Res. 106 (2016) 272–282.
[2] E. Hosseinipour, K. Park, L. Burlace, T. Naughton, P.A. Davies, A free-piston batch reverse osmosis (RO) system for brackish water desalination: experimental study and model validation, Desalination 527 (2022) 115524.
[3] A. Das, A.K. Rao, S. Alnajdi, D.M. Warsinger, Pressure exchanger batch reverse osmosis with zero downtime operation, Desalination 574 (2024) 117121.
[4] E. Hosseinipour, E. Harris, H.A. El Nazer, Y.M.A. Mohamed, P.A. Davies, Desalination by batch reverse osmosis (RO) of brackish groundwater containing sparingly soluble salts, Desalination 566 (2023) 116875.
[5] A. Das, A. Naderi Beni, C. Bernal-Botero, D.M. Warsinger, Temporally multi-staged batch counterflow reverse osmosis, Desalination 575 (2024) 117238.
[6] H. Abu Ali, M. Baronian, L. Burlace, P.A. Davies, S. Halasah, M. Hind, A. Hossain, C. Lipchin, A. Majali, M. Mark, T. Naughton, Off-grid desalination for irrigation in the Jordan Valley, Desalinaation and Water Treatment 168 (2019) 143–154.
[7] S. Cordoba, A. Das, J. Leon, J.M. Garcia, D.M. Warsinger, Double-acting batch reverse osmosis configuration for best-in-class efficiency and low downtime, Desalination 506 (2021) 114959.
[8] P.A. Davies, J. Wayman, C. Alatta, K. Nguyen, J. Orfi, A desalination system with efficiency approaching the theoretical limits, Desalin. Water Treat. 57 (2016) 23206–23216.
[9] J.R. Werber, A. Deshmukh, M. Elimelech, Can batch or semi-batch processes save energy in reverse-osmosis desalination? Desalination 402 (2017) 109–122.
[10] K. Park, P.A. Davies, A compact hybrid batch/semi-batch reverse osmosis (HBSRO) system for high-recovery, low-energy desalination, Desalination 504 (2021) 114976.
[11] E. Hosseinipour, S. Karimi, S. Barbe, K. Park, P.A. Davies, Hybrid semi-batch/batch reverse osmosis (HSBRO) for use in zero liquid discharge (ZLD) applications, Desalination 544 (2022) 116126.
[12] B.R. Babu, S.U. Bhanu, K.S. Meera, Waste minimization in electroplating industries: a review, J. Environ. Sci. Health C 27 (2009) 155–177.
[13] E. Vaiopoulou, P. Gikas, Regulations for chromium emissions to the aquatic environment in Europe and elsewhere, Chemosphere 254 (2020) 126876.
[14] S.S. Hosseini, E. Bringas, N.R. Tan, I. Ortiz, M. Ghahramani, M.A.A. Shahmirzadi, Recent progress in development of high performance polymeric membranes and materials for metal plating wastewater treatment: a review, journal of water, Process. Eng. 9 (2016) 78–110.
[15] https://www.zvo.org/publikationen/jahresbericht/, access date: 12-02-2024.
[16] https://www.zvo.org/indizes/rohstoffpreisindex-verchromung, access date: 12-02-2024.
[17] Commission Regulation (EU) No. 348/2013 of 17 April 2013 amending Annex XIV to regulation (EC) No. 1907/2006 of the European parliament and of the council on the registration, evaluation, authorisation and restriction of chemicals (REACH). Off. J. Eur. Union 2013, L108, 1–5.
[18] A. Pechova, L. Pavlata, Chromium as an essential nutrient: a review, Vet. Med. 52 (2007) 1.
[19] R. Engstler, J. Reipert, S. Karimi, J.L. Vukušić, F. Heinzler, P. Davies, M. Ulbricht, S. Barbe, A reverse osmosis process to recover and recycle trivalent chromium from electroplating wastewater, Membranes 12 (2022) 853.
[20] M. Leimbach, C. Tschaar, D. Zapf, M. Kurniawan, U. Schmidt, A. Bund, Relation between color and surface morphology of electrodeposited chromium for decorative applications, J. Electrochem. Soc. 166 (2019) D205.
[21] L. Büker, R. Dickbreder, R. Böttcher, S. Sadowski, A. Bund, Investigation of the reaction kinetics of chromium(III) ions with carboxylic acids in aqueous solutions and the associated effects on chromium deposition, J. Electrochem. Soc. 167 (2020) 162509.
[22] Y. Xia, J. Yu, S. Jin, Q. Cheng, Performance analysis of electroplating wastewater treatment system combining air compression expansion cycle with spray drying tower, Appl. Therm. Eng. 184 (2021) 116257.
[23] J. Yang, C. Zhang, Z. Zhang, L. Yang, Electroplating wastewater concentration system utilizing mechanical vapor recompression, J. Environ. Eng. 144 (2018) 04018053.
[24] M.T. Kamar, H. Elattar, A.S. Mahmoud, R.W. Peters, M.K. Mostafa, A critical review of state-of-the-art technologies for electroplating wastewater treatment, Int. J. Environ. Anal. Chem. (2022) 1–34.

[25] A.A. Azmi, J. Jai, N.A. Zamanhuri, A. Yahya, Precious metals recovery from electroplating wastewater: a review, IOP Conference Series: Materials Science and Engineering 358 (2018) 012024.
[26] K. Staszak, I. Kruszelnicka, D. Ginter-Kramarczyk, W. Góra, M. Baraniak, G. Lota, M. Regel-Rosocka, Advances in the removal of Cr(III), from Spent Industrial Effluents: A Review, in, Materials 16 (2023) 378.
[27] I. Frenzel, D.F. Stamatialis, M. Wessling, Water recycling from mixed chromic acid waste effluents by membrane technology, Sep. Purif. Technol. 49 (2006) 76–83.
[28] E. Piedra, J.R. Álvarez, S. Luque, Hexavalent chromium removal from chromium plating rinsing water with membrane technology, Desalin. Water Treat. 53 (2015) 1431–1439.
[29] S. Chung, S. Kim, J.-O. Kim, J. Chung, Feasibility of Combining Reverse Osmosis–Ferrite Process for Reclamation of Metal Plating Wastewater and Recovery of Heavy Metals, Ind. Eng. Chem. Res. 53 (2014) 15192–15199.
[30] I. Petrinic, J. Korenak, D. Povodnik, C. Hélix-Nielsen, A feasibility study of ultrafiltration/reverse osmosis (UF/RO)-based wastewater treatment and reuse in the metal finishing industry, J. Clean. Prod. 101 (2015) 292–300.
[31] J. Schoeman, J. Van Staden, H. Saayman, W. Vorster, Evaluation of reverse osmosis for electroplating effluent treatment, Water Sci. Technol. 25 (1992) 79–93.
[32] J. Walker Jr., J. Wilson, C. Brown Jr., Minimization of chromium-contaminated wastewater at a plating facility in the eastern United States, Environ. Prog. 9 (1990) 156–160.
[33] N. Voutchkov, Energy use for membrane seawater desalination – current status and trends, Desalination 431 (2018) 2–14.
[34] D. Cingolani, F. Fatone, N. Frison, M. Spinelli, A.L. Eusebi, Pilot-scale multi-stage reverse osmosis (DT-RO) for water recovery from landfill leachate, Waste Manag. 76 (2018) 566–574.
[35] Q.J. Wei, C.I. Tucker, P.J. Wu, A.M. Trueworthy, E.W. Tow, J.H. Lienhard, Impact of salt retention on true batch reverse osmosis energy consumption: experiments and model validation, Desalination 479 (2020) 114177.
[36] https://buttondown.email/harmonyDesalting/archive/harmony-team-demonstrates-batch-ro-in-the-field/, access date: 12-02-2024.
[37] P. Davies, T. Naughton, L. Burlace, K. Park, Desalination system and method, in: Internation Application Published Under the Patent Cooperation Treaty, PCT, 2022.
[38] D.M. Davenport, A. Deshmukh, J.R. Werber, M. Elimelech, High-pressure reverse osmosis for energy-efficient hypersaline brine desalination: current status, design considerations, and research needs, Environ. Sci. Technol. Lett. 5 (2018) 467–475.
[39] TRILYTE (R) FLASH SF, MacDermid Enthone, MDS number: 997301019/2, Process code: 081009/001 in: Technical data sheet, MacDermid Enthone, 2019.
[40] https://industrial.macdermidenthone.com/application/files/5215/7061/3130/TRILYTE_FLASH_SF_MEIS_B76_2018_1804.pdf, access date: 12-02-2024.
[41] Regulatory.DE@Macdermid.com, SAFETY DATA SHEET for TRILYTE Flash SF make-up in: Safety Data Sheet, MacDermid Performance Solutions UK Limited, 2020.
[42] R. Engstler, S. Barbe, S.J. Bohr, P. Davies, S. Karimi, I. Hosseinipour, A. Sapalidis, Deliverable 3.3- Lab scale HRRO/IX unit, in: Project title: Intelligent Water Treatment for water preservation combined with simultaneous energy production and material recovery in energy intensive industries, Grant Agreement Number, 2021, p. 958454.
[43] Regulatory.DE@Macdermid.com, TRILYTE Flash SF Buffer in: Safety data sheet, MacDermid Performance Solutions UK Limited, 2021.
[44] Regulatory.DE@Macdermid.com, TRILYTE Flash SF Replenisher in: Safety data sheet, MacDermid Performance Solutions UK Limited, 2021TRILYTE Flash SF Replenisher.
[45] Regulatory.DE@Macdermid.com, TRILYTE Wetting Agent in: Safety Data Sheet, MacDermid Performance Solutions UK Limited, 2021.
[46] X. Jin, C.Y. Tang, Y. Gu, Q. She, S. Qi, Boric acid permeation in forward osmosis membrane processes: modeling, experiments, and implications, Environ. Sci. Technol. 45 (2011) 2323–2330.
[47] Y. Cengeloglu, G. Arslan, A. Tor, I. Kocak, N. Dursun, Removal of boron from water by using reverse osmosis, Sep. Purif. Technol. 64 (2008) 141–146.
[48] M. Li, Effects of finite flux and flushing efficacy on specific energy consumption in semi-batch and batch reverse osmosis processes, Desalination 496 (2020) 114646.
[49] S. Nakaya, A. Yamamoto, T. Kawanishi, N. Toya, H. Miyakawa, K. Takeuchi, M. Endo, Detection of dynamic biofouling from adenosine triphosphate measurements in water concentrated from reverse osmosis desalination of seawater, Desalination 518 (2021) 115286.
[50] D.M. Warsinger, E.W. Tow, L.A. Maswadeh, G.B. Connors, J. Swaminathan, J. H. Lienhard V, Inorganic fouling mitigation by salinity cycling in batch reverse osmosis, Water Res. 137 (2018) 384–394.
[51] T. Tong, M. Elimelech, The global rise of zero liquid discharge for wastewater management: drivers, technologies, and future directions, Environ. Sci. Technol. 50 (2016) 6846–6855.
[52] Y. Muhammad, W. Lee, Zero-liquid discharge (ZLD) technology for resource recovery from wastewater: a review, Sci. Total Environ. 681 (2019) 551–563.
[53] E. Hosseinipour, P.A. Davies, Effect of membrane properties on the performance of batch reverse osmosis (RO): the potential to minimize energy consumption, Desalination 577 (2024) 117378.